IEEE Photonics Journal
An IEEE Photonics Society Publication

Open Access

# Arbitrary Waveform Generation Based on Dispersion-Free Wavelength-to-Time Mapping Technique

Volume 10, Number 1, February 2018

Xinyi Zhu
Hao Sun
Wei Li
Ninghua Zhu
Ming Li

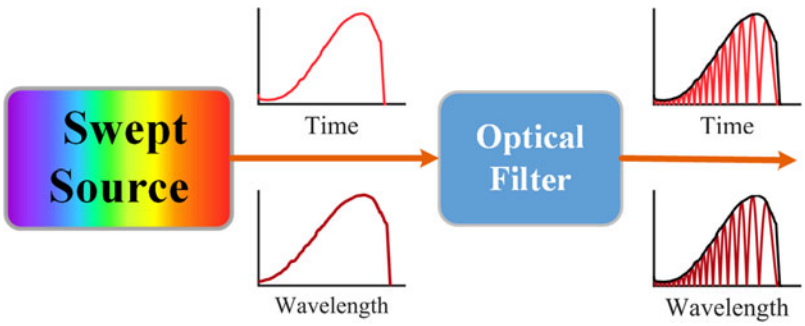


DOI: 10.1109/JPHOT.2018.2798610
1943-0655 © 2018 IEEE

IEEE photonics SOCIETY

IEEE

# Arbitrary Waveform Generation Based on Dispersion-Free Wavelength-to-Time Mapping Technique

**Xinyi Zhu**,[1,2] **Hao Sun**,[1,2] **Wei Li**,[1,2] **Ninghua Zhu**,[1,2] **and Ming Li** [1,2]

[1]Institute of Semiconductors, Chinese Academy of Sciences, no. 35, Tsinghua East Road, Beijing 100083, China
[2]School of Electronic, Electrical and Communication Engineering, University of Chinese Academy of Sciences, Beijing 100049, China

*DOI:10.1109/JPHOT.2018.2798610*
*1943-0655 © 2018 IEEE.Translations and content mining are permitted for academic research only. Personal use is also permitted, but republication/redistribution requires IEEE permission. See http://www.ieee.org/publications standards/publications/rights/index.html for more information.*

Manuscript received December 26, 2017; revised January 15, 2018; accepted January 22, 2018. Date of publication January 29, 2018; date of current version February 22, 2018. This work was supported in part by the National Natural Science Foundation of China under Grant 61522509, Grant 61377002, and Grant 61090391); in part by the National High-Tech Research and Development Program of China under Grant 2015AA017102. The work of M. Li was supported partly by the Thousand Young Talent Program. Corresponding author: Ming Li (e-mail: ml@semi.ac.cn).

**Abstract:** We proposed and experimentally demonstrated an approach of dispersion-free arbitrary waveform generation based on a wavelength-swept laser, for the first time to the best of our knowledge. The system has been proven to generate a variety of waveforms, such as Gaussian pulses, rectangular pulses, and a chirped pulse with a large time-bandwidth product of 273.6. Thanks to the linear relationship of frequency to the time of the wavelength-swept laser, time-domain optical signal exhibits the user-defined shape of the optical spectrum without any dispersive element. Furthermore, the proposed method features simple structure, full reconfiguration, and, especially, the high potential for integration.

**Index Terms:** Pulse shaping, microwave photonics, arbitrary waveform generation (AWG).

## 1. Introduction

Techniques for synthesis of arbitrary waveform in optical domain have been attracting persistent attention for numerous applications, including the modern radar, medical imaging, ultrafast chemical reactions, sensor networks and optical coherence tomography [1]–[4]. Compared with its electrical counterparts, this perspective offers a promising solution for its prominent features, such as immunity to electromagnetic interference (EMI), low loss, simple structure, and reconfigurability [5].

Plenty of methods have been proposed and experimentally demonstrated, such as direct space-to-time pulse shaping [6]–[8], temporal pulse shaping (TPS) [9], [10], spectral-shaping and wavelength-to-time mapping (SS-WTTM) [11]–[13], etc. Among these approaches, SS-WTTM solution is a very simple and promising alternative. However, in order to map the optical spectrum into time domain, it always needs a dispersive element, in which different frequency components have different speeds. Therefore, the dispersive elements, such as a fiber Bragg grating [14] or a long spool of optical fiber [15], are essential in the AWG system that provide wavelength-to-time mapping (WTTM). Unfortunately, the on-chip dispersive elements with a large group velocity dispersion (GVD) will cause long waveguides and high propagation loss. For example, the dispersion

of a 5.5 km single mode fiber (SMF) is equal to the dispersion of a 21-m-long silicon waveguide with the GVD of 4400 ps/(nm · km) [16]. Fiber Bragg gratings can provide strong dispersion, while its limited delay-bandwidth product would restrict the application in integration [16]. Thus, the main challenge of integrating the whole AWG system is to achieve an on-chip dispersive medium with a large GVD which is indispensable in the conventional WTTM process.

Most reported on-chip AWG methods are based on integrated optical filters. The optical filters can be micro-rings [15], linearly chirped waveguide gratings [17], [18] or a Mach-Zehnder interferometer structure [19]. In [15], several integrated rings are implemented as the optical filter. The resonant wavelength of each ring is tuned by a micro-heater. Key features of this approach is the high instantaneous bandwidth and the flexible frequency band. To realize the WTTM, a 5.5 km SMF is needed outside the chip. Similarly, other works based on integrated optical filters [15]–[19] also use extra SMF or dispersion compensating fiber (DCF) to stretch the optical signal, which is called WTTM. In order to break through this bottleneck, the on-chip optical delay line is an admirable option [16], where optical signals with different wavelengths can be separated in time domain by controlling the delay.

In this paper, we introduce a novel method of AWG with dispersion-free WTTM technique, which is based on a wavelength-swept laser. The linear frequency-swept characteristic of the swept laser offers the possibility of obtaining several different waveforms directly after a high-speed photodetector (PD), eliminating the demand for large dispersion. It is interesting to note that the target waveform can be easily controlled by a user-defined optical spectral shaper, which shows the flexibility. Moreover, numerous works on integrated reconfigurable optical filters [20]–[22] and wavelength-swept lasers [23]–[30] have been reported. On the basis of tunable characteristic of distributed feedback (DFB) laser [23], [25], some experiments achieved 10 nm wavelength sweep range with the repetition rate exceeding tens of kilohertz [25]. For another, analyses and experiments of distributed Bragg reflector (DBR) lasers tuning performance are presented in [26]. Furthermore, a monolithic semiconductor device based on Vernier-Tuned Distributed Bragg Reector (VT-DBR) enables high-speed sweep with over 99% duty cycle [27], [28]. Recently, several other methods of swept source have attracted many attentions, involving vertical-cavity surface emitting laser (VCSEL) [29] and some analyses of the integrated Fourier-domain mode locking laser [30]. Based on these integrated photonic devices which show the availability of integrated swept sources, our proposed method possesses the high possibility of integration.

## 2. Principle

Fig. 1(a) shows the conventional system of AWG based on WTTM. A short-pulse laser with large bandwidth firstly passes through a high dispersion to stretch its spectrum. Then an optical filter is used to tailor it thus the temporal waveform would have the same shape as the optical spectrum. Nevertheless, it is clearly that the dispersive device is bulky and will bring large cost. In our system, a wavelength-swept laser is implemented to replace the short-pulse laser and the large dispersion used to realize WTTM. Therefore, to generate arbitrary waveform, we only need a swept source and an optical filter. Fig. 1(b) shows the simple schematic highlighting the fundamental concept of our method. Here, a Fourier domain mode locking (FDML) laser is applied as the frequency-swept optical source. A high-speed, frequency-swept optical light from the swept laser is shaped by an optical spectral filter. Thanks to the linear frequency-to-time relationship of the wavelength-swept laser, the shaped optical spectrum has the same envelope as the temporal waveform. Thus the process of WTTM is realized.

Due to the sinusoidally driven filter, the frequency of the laser varies sinusoidally rather than linearly with time [32]. However, the maximum bandwidth of our optical spectral filter is only 40 nm, which is much smaller than the swept range of the laser, so that the relationship of frequency to time can be approximately considered as linear but with a slight deviation. Here, we analyze the system in one period $T$ as each period is equivalent. We assume the starting time of the period is at $t = 0$ and in consideration of the scanning mode, the output wavelength versus time can be

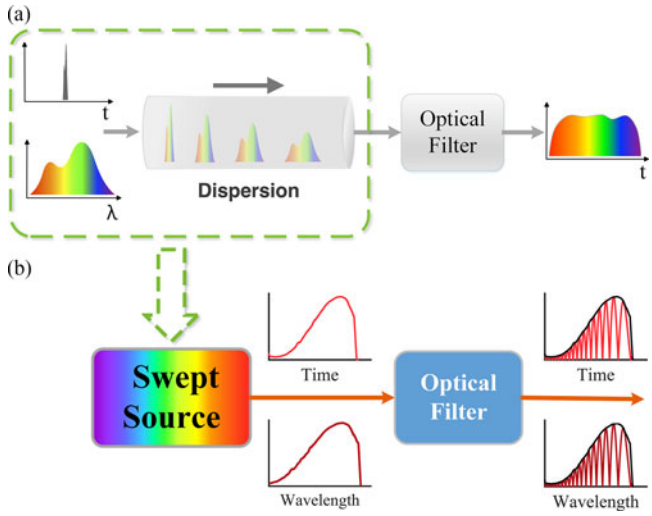


Fig. 1. (a) The conventional AWG system based on WTTM. (b) Schematic diagram of our proposed method based on a swept source.

expressed as

$$\lambda(t) = -kt + \lambda_0, 0 < t < T, \tag{1}$$

where $\lambda_0$ is the starting wavelength of the swept range and the ratio $k$ is constant. The minus sign represents the scanning mode which is backward wavelength-swept (longer to shorter wavelengths). As a result, the direction of the temporal envelope and the spectrum is inverse. To better express the ratio $k$, we give the relation between the bandwidth and the temporal duration of the optical signal

$$\Delta\lambda = -k \cdot \Delta t. \tag{2}$$

Considering the output of the laser, $\Delta t$ denotes the temporal duration which is also the period, corresponding to the reciprocal of the repetition rate of our swept laser. And $\Delta\lambda$ is the swept wavelength range. Thus, the ratio $k$ can be calculated from the parameters of the laser.

We define the output energy spectrum of the swept-laser as $S_{in}(\lambda)$. Therefore, in the proportion to spectrum shown in (1), the intensity of the temporal waveform can be expressed as $s_{in}(t) = S_{in}(\lambda)_{\lambda=-kt+\lambda_0}$. Notice that the wavelength of the laser varies linearly with time. For simplicity, we assume the transfer function of the optical spectral filter is $H(\lambda)$. Thus, after propagating through the filter, the intensity of the shaped optical spectrum is

$$X_{out}(\lambda) = S_{in}(\lambda) |H(\lambda)|^2. \tag{3}$$

Due to the linear relationship of wavelength to time in the swept laser, the envelope of the detected temporal waveform is a scaled replica of the shaped optical spectrum according to (1), which is given by

$$I(t) \propto X_{out}(\lambda)_{\lambda=-kt+\lambda_0}. \tag{4}$$

Consequently, the input optical energy spectrum is linearly mapped into the time-domain with a scaled factor $\lambda = -kt + \lambda_0$. The so-called linear WTTM is induced by using the frequency-swept laser without GVDs. Based on this concept, scaled factor $k$ can be changed by tuning the swept range and slightly controlling the repetition rate of the wavelength-swept laser. The wavelength swept range of our laser can be changed from 55 nm to 140 nm and the repetition rate as well as the central wavelength can only be finely tuned according to the wavelength range. In addition, the generated signal can be easily reconstructed by programming the user-defined optical filter.

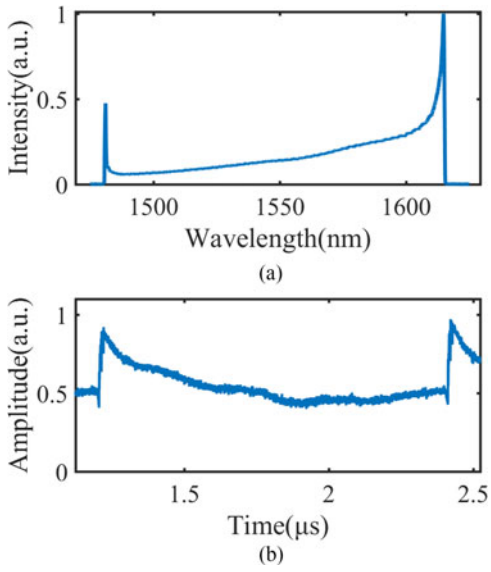


Fig. 2. (a) The measured optical spectrum of the swept laser and, (b) the temporal waveform.

As is known that the maximum frequency $f_{max}$ of the generated radio-frequency (RF) signal is inversely related to the temporal resolution $\delta t$ of it [12]. We assume the free spectrum range (FSR) of the swept source is smaller than the optical spectrum resolution of the optical filter. For our swept laser, the FSR is related to the repetition rate, which is around 828.49 kHz. The FSR of the laser is quite small compared with current optical filters [20]–[22]. Therefore, according to (2), the bandwidth of the output signal can be written as

$$f_{max} \sim \frac{1}{\delta t} = \frac{k}{\delta \lambda}. \tag{5}$$

where $\delta\lambda$ denotes the spectral resolution of the filtered optical signal. Based on these analyses, the maximum frequency of the generated signal is mostly determined by the spectral resolution of the optical filter and the ratio $k$. The speed of the PD can also influence the maximum frequency. For example, if the FSR of the filter is 500, MHz and according to (5), $f_{max}$ of the generated signal should be around 29 GHz. Whereas, it would be limited by the PD, the speed of which is 18 GHz.

## 3. Experimental Results

In the experiment, the swept range of the laser is set as 140 nm with the repetition rate of 828.49 kHz. The output power is around 14 dBm. Notice that the output power can be tuned up to 14 dB by adjusting the current of the laser. According to (2), the period of the output is $\Delta t = 1/(828.49\ \text{kHz}) = 1.21 \times 10^3$ ns and the ratio $k$ can be calculated as $k = 140\ \text{nm}/\left(1.21 \times 10^3\ \text{ns}\right) \approx 0.116$ nm/ns. The measured optical spectrum with linear scale and the temporal waveform of the laser are shown in Fig. 2. The output of the swept laser is a frequency-swept light and its wavelength changes rapidly and periodically with time, which has nearly constant amplitude and 100% duty cycle. Unlike the standard mode locking laser, the output of the swept laser is not a train of short pulses; instead, it is a train of frequency-swept or highly chirped, very long pulses [31]. Then the output of the laser goes through an optical filter as the principle shows. The resolution of our filter is 10 GHz and the operating frequency range is 1527.4 nm $\sim$ 1567.5 nm (FINISAR WaveShaper 4000s). Moreover, the response of the optical spectral filter can be tuned in real time by flexible designing.

We first select Gaussian pulses with different full widths at half maximum (FWHMs) centered at 1553.2 nm. By proper controlling the optical spectral filter, three different Gaussian pulses are generated and the shaped optical spectrums are measured by an optical spectrum analyzer (OSA),

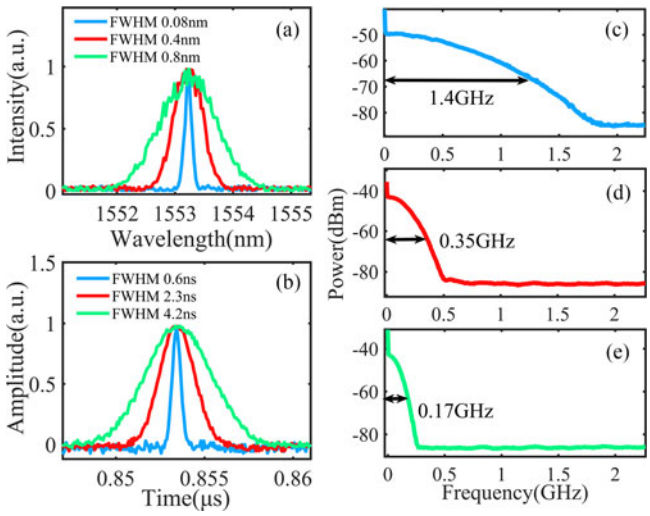


Fig. 3. Experimental results. (a) Filtered optical spectrums of Gaussian pulses with different full width at half maximum (FWHM). (b) The generated signals in time domain. (c)–(e) Corresponding spectrums of the output signals. Note that the measured optical spectrums, temporal waveforms and the spectrums of the same output signals are plotted with the same color.

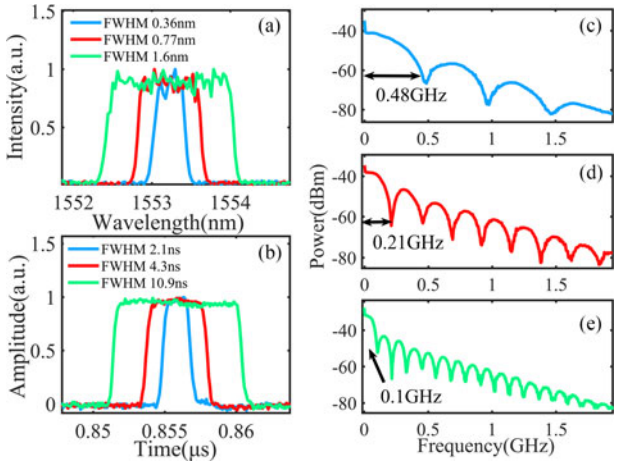


Fig. 4. (a) The shaped optical spectrums of rectangular pulses. (b) Temporal waveforms and (c)–(e) measured spectrums of generated signals.

shown in Fig. 3(a). The FWHMs of the three filtered optical spectrums are 0.08 nm, 0.4 nm and 0.8 nm, which agree well with our settings of the programmable optical filter. In order to better present the linear mapping relationship, the measured optical spectrum is plotted with linear scales. Temporal waveforms are captured by implementing a real-time oscilloscope with the sampling rate of 12.5 Gs/s, shown in Fig. 3(b), where the FWHMs of the temporal pulses are 0.6 ns, 2.3 ns, and 4.2 ns, respectively. It is obvious that the generated pulse has a Gaussian shape both in temporal domain and frequency domain. Also, the spectrums of the generated signals are measured by a Spectrum Analyzer (RBW $=$ 1 MHz) (see Fig. 3(c)–(e)) and the bandwidths are around 1.4 GHz, 0.35 GHz and 0.17 GHz, which meets the relation between the maximum frequency $f_{max}$ and temporal resolution $\delta t$ of the signal ((5)). Note that the experimental results are measured in single shoot.

In order to verify the reconfigurability, rectangular waveforms with different FWHMs are achieved. The measured optical spectrums and temporal waveforms are shown in Fig. 4(a) and (b),

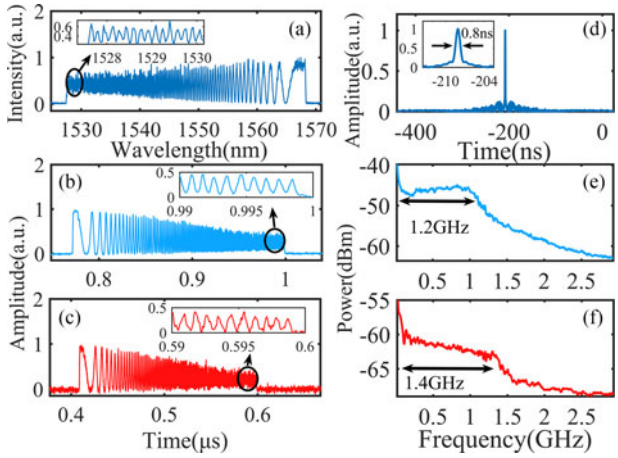


Fig. 5. (a) Optical spectrums of the chirped pulses and, (b) temporal waveforms (inset: zoom-in display). (c) Measured waveforms of the compressed chirped signals by a 55.5 km SMF. (d) The compressed waveform by autocorrelation. (e) The measured spectrums of the generated chirped signals in (b). (f)The spectrums of the compressed signals in (c).

respectively. The FWHMs of the optical spectrums are 0.36 nm, 0.77 nm, and 1.6 nm and temporal widths of the generated signals are 2.1 ns, 4.3 ns, and 10.9 ns, which matches well with the prediction. Fig. 4(c)–(e) depict the spectrums which should be sinc functions, and the bandwidths of the main lobes are 0.48 GHz, 0.21 GHz and 0.1 GHz, respectively.

Furthermore, we show the capability of generating chirped pulse by programming the response of the optical spectral filter, as shown in Fig. 5(a). The wavelength ranges from 1527.4 nm to 1567.5 nm which is the maximum operating range of the optical spectral filter. Based on the frequency-to-time mapping law, the temporal waveform can be obtained and has the same profile as the shaped spectrum but with an inverse direction, shown in Fig. 5(b). The chirped pulse waveform has a temporal duration of 228 ns. According to Fig. 5(e), the 3 dB bandwidth of the chirped signal is around 1.2 GHz and the time-bandwidth product (TBWP) is also calculated, $TBWP = B_f \cdot \Delta T = 228\ \text{ns} \cdot 1.2\ \text{GHz} = 273.6$, which is much higher than previous works [13], [14]. From an autocorrelation operation, we have the compressed pulse with a FWHM of 0.8 ns (see in Fig. 5(d)). Therefore, the pulse compression ratio is around 285.

We also evaluated the compressibility of the chirped pulse. Considering the backward-swept characteristic of our swept laser mentioned before and the GVD of the single-mode fiber (SMF), a 55.5 km SMF is employed. Fig. 5(c) exhibits the output signal measured by using a real-time oscilloscope. The temporal duration of the chirped signal is compressed to 190ns. Meanwhile, the bandwidth of the chirped pulse is around 1.4 GHz (see in Fig. 5(f)), corresponding to a compression ratio of 1.2. The compression time is $\delta t = 17\ \text{ps}/\ (\text{nm} \cdot \text{km}) \cdot 55.5\ \text{km} \cdot 40\ \text{nm} = 37.74\ \text{ns}$. However, since the temporal duration of the chirped signal is large (228 ns), the compressed result is not obvious. The propagation loss of the long fiber would also limit our compression. As a result, to achieve a larger compression ratio, a longer SMF and some optical amplifiers need to be implemented to compensate for the optical loss. Also, the calculated signal-to-noise-ratios (SNRs) of the generated signals are shown in Fig. 6. It can be seen the SNRs are around 30 dB. The SNR represents the quality of the generated signals, which is mainly determined by the noise of the laser, the power loss of the optical filter and the noise of the photodetector. Because of the propagation loss in the SMF, the SNR of the compressed signal is lower, which is 19.6 dB.

## 4. Discussion

Comparing to conventional AWG techniques, the frequency of the generated signal in this system is much lower because of the lower repetition rate of the laser and the lower resolution of our optical

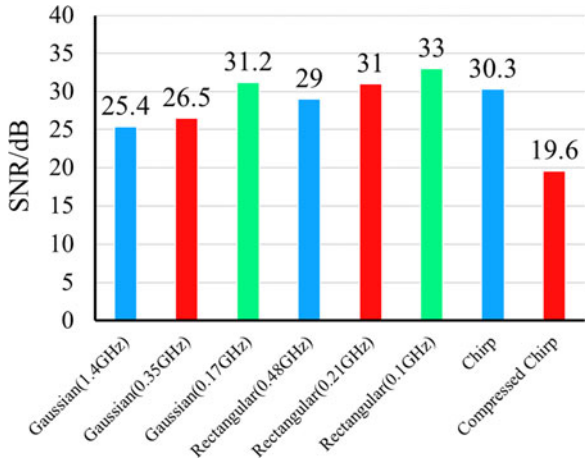


Fig. 6. The calculated SNRs of the generated signals.

filter. Thus, in order to obtain a higher frequency, it requires an optical spectral filter with a higher spectral resolution. Nevertheless, the swept laser offers a large temporal duration which shows a potential of much higher TBWP of the chirped pulse, which would have a good performance in radar. And if a higher spectral resolution of the on-chip optical filter is available, for example, 2 GHz [21], the bandwidth of the chirped pulse would be probably up to around 5 GHz, according to (5), and TBWP can be as high as 1255. On the other hand, since the repetition rate is lower than the mode-locked lasers (tens of MHz), the duration of the generated signal would be much longer. That is to say, the output has a lower pulse repetition frequency (PRF). In the pulse Doppler radar system, a high-PRF radar has a good performance with unambiguous velocity, while in a low-PRF or a medium-PRF (e. g. 12 kHz), the ranges of targets have less eclipsing than in high PRF [35]. Also, the signal with longer duration would contribute to a larger detection range. Hence, the generated signal with a repetition rate around 800 kHz in our proposal could be used in the pulse Doppler radar for detection.

Dispersive elements, such as long optical fibers (5.5 km [15]) or fiber Bragg gratings, are indispensable in the conventional AWG system to provide various time delays of different wavelengths, called WTTM. However, integration of these elements would lead to incredible long waveguides and insertion loss. Our proposal can solve this problem by using a wavelength-swept source to supply a linear relationship of frequency to time. Consequently, it has a high potential to realize the fully integrated AWG because no dispersive element is needed. Fortunately, this can be easily achieved according to previous works. For example, an all-semiconductor, all-electronic tunable and compact swept laser that can be user-controlled by software has been reported [28]. The laser has a wide swept range of 40 nm with repetition rate varying from 20 kHz to 200 kHz which has a similar characteristic of our swept laser. A MEMS tunable VCSEL with adjustable repetition rate (50 kHz $\sim$ 580 kHz) and adjustable swept range [29], as well as a DFB laser with 10 nm swept range and over tens of kilohertz speed [25] can also act as the swept source. Moreover, an integrated FDML laser has been theoretically investigated recently [30] which shows the potential of the application of integrated FDML laser in the future. Therefore, the main device of our proposal can be realized by an integrated swept laser, showing the high speed and wide swept range. The optical filter is another significant device. The performance of the programmable optical filter can be improved by using a two-dimensional photonic silicon waveguide mesh. It can realize over twenty different functionalities by programming [20]. Also, a narrowband reconfigurable photonics filter has been obtained by using a silicon-on-insulator waveguide and the FSR is 2 GHz [21]. As for the integrated photodetectors, a recent study has shown the possibility to obtain an integrated ultrafast photodetector with high responsivity by using graphene and its response rate exceeds 20 GHz

[33]. Also, an InP-based waveguide-integrated photodetector with 100 GHz bandwidth has been reported [34].

## 5. Conclusion

In conclusion, a novel approach of achieving AWG based on WTTM with a wavelength-swept laser has been proposed and experimentally demonstrated. At the same time, the reconfigurablity of this technique has also been verified by synthesizing different waveforms as user defined. It is worth to note that our experiment is limited by on-chip devices, but with the availability of integrated swept sources [22]–[29] and tunable optical filters [19]–[21], an integrated optical AWG could be achieved based on our proposed concept. Therefore, the adoption of the frequency-swept laser opens a new window for integrated AWG because no GVD is needed in this method. Thus, the proposed technique offers prospect not only for AWG with a simple structure or a high reconfigurability, but also for high possibility of integration.

## Acknowledgment

We acknowledge S. Sun, J. Tang, N. Shi, and T. Hao for comments and discussion.

## References

[1] J. Capmany and D. Novak, "Microwave photonics combines two worlds," *Nature Photon.*, vol. 1 no. 6, pp. 319–330, 2007.
[2] W Wei, Li Yi, Y Jaoun, and W Hu, "Software-defined microwave photonic filter with high reconfigurable resolution," *Sci. Rep.* vol. 6, 2016, Art. no. 35621.
[3] M. Li and J. Yao, "Photonic generation of continuously tunable chirped microwave waveforms based on a temporal interferometer incorporating an optically pumped linearly chirped fiber Bragg grating," *IEEE Trans. Microw. Theory Tech.*, vol. 59 no. 12, pp. 3531–3537, Dec. 2011.
[4] P. C. Chou, H. A. Haus, and J. F. Brennan, "Reconfigurable time-domain spectral shaping of an optical pulse stretched by a fiber Bragg grating," *Opt. Lett.*, vol. 25 no. 8, pp. 524–526, 2000.
[5] H. Zmuda and E. N. Toughlian, *Photonic Aspects of Modern Radar.* Norwood, MA, USA: Artech House, 1994.
[6] D. E. Leaird and A. M. Weiner, "Femtosecond optical packet generation by a direct space-to-time pulse shaper," *Opt. Lett.*, vol. 24 no. 12, pp. 853–855, 1999.
[7] J. D. McKinney, D. E. Leaird, and A. M. Weiner, "Millimeter-wave arbitrary waveform generation with a direct space-to-time pulse shaper," *Opt. Lett.*, vol. 27 no. 15, pp. 1345–1347, 2002.
[8] R. Ashrafi, M. Li, S. Larochelle, and J. Azaa, "Superluminal space-to-time mapping in grating-assisted co-directional couplers," *Opt Exp.*, vol. 21 no. 5, pp. 6249–6256, 2013.
[9] M. Li, Y. Han, S. Pan, and J. Yao, "Experimental demonstration of symmetrical waveform generation based on amplitude-only modulation in a fiber-based temporal pulse shaping system," *IEEE Photon. Technol. Lett.*, vol. 23 no. 11, pp. 715–717, Jun. 2011.
[10] J. Azaa, N. K. Berger, B. Levit, and B. Fischer, "Reconfigurable generation of high-repetition-rate optical pulse sequences based on time domain phase-only filtering," *Opt. Lett.*, vol. 30 no. 23, pp. 3228–3230, 2005.
[11] M. Li, L. Y. Shao, J. Albert, and J. Yao, "Tilted fiber Bragg grating for chirped microwave waveform generation," *IEEE Photon. Technol. Lett.*, vol. 23 no. 5, pp. 314–316, Mar. 2011.
[12] A. Dezfooliyan and A. M. Weiner, "Photonic synthesis of high fidelity microwave arbitrary waveforms using near field frequency to time mapping," *Opt Exp.*, vol. 21 no. 19, pp. 22974–22987, 2013.
[13] M. Rius, M. Bolea, J. Mora, and J. Capmany, "Incoherent photonic processing for chirped microwave pulse generation," *IEEE Photon. Technol. Lett.*, vol. 29 no. 1, pp. 7–10, Jan. 2017.
[14] C. Wang and J. Yao, "Photonic generation of chirped millimeter-wave pulses based on nonlinear frequency-to-time mapping in a nonlinearly chirped fiber Bragg grating," *IEEE Trans. Microw. Theory Tech.*, vol. 56 no. 2, pp. 542–553, Feb. 2008.
[15] M. H. Khan *et al.*, "Ultrabroad-bandwidth arbitrary radiofrequency waveform generation with a silicon photonic chip-based spectral shaper," *Nature Photon.*, vol. 4 no. 2, pp. 117–122, 2010.
[16] J. Wang *et al.*, "Reconfigurable radio-frequency arbitrary waveforms synthesized in a silicon photonic chip," *Nature Commun.* vol. 6, p. 5957, 2015.
[17] W. Zhang and J. Yao, "Photonic generation of linearly chirped microwave waveforms using a silicon-based on-chip spectral shaper incorporating two linearly chirped waveguide Bragg gratings," *J. Lightw. Technol.*, vol. 33 no. 24, pp. 5047–5054, Dec. 2015.
[18] S. Liao *et al.*, "Arbitrary waveform generator and differentiator employing an integrated optical pulse shaper," *Opt Exp.*, vol. 23 no. 9, pp. 12161–12173, 2015.
[19] S. Yan *et al.*, "Photonic linear chirped microwave signal generation based on the ultra-compact spectral shaper using the slow light effect," *Opt. Lett.*, vol. 42 no. 17, pp. 3299–3302, 2017.
[20] D. Prez *et al.*, "Multipurpose silicon photonics signal processor core," *Nature Commun.* vol. 8, no. 1, p. 636, 2017.

[21] N. Feng *et al.*, "Thermally-efficient reconfigurable narrowband RF-photonic filter," *Opt Exp.*, vol. 18 no. 24, pp. 24648–24653, 2010.
[22] J. S. Fandio, P. Muoz, D. Domnech, and J. Capmany, "A monolithic integrated photonic microwave filter," *Nature Photon.* vol. 11, pp. 124–129, 2017.
[23] G. Morthier and P. Vankwikelberge, *Handbook of Distributed Feedback Laser Diodes*, 2nd ed. Norwood, MA, USA: Artech House, 2013.
[24] J. Buus, M. C. Amann, and D. J. Blumenthal, Tunable laser diodes and related optical sources, 2nd ed. Hoboken, NJ , USA: Wiley, 2005.
[25] M. Njegovec and D. Donlagic, "Rapid and broad wavelength sweeping of standard telecommunication distributed feedback laser diode," *Opt. Lett.*, vol. 38 no. 11, pp. 1999–2001, 2013.
[26] M. Teshima, "Dynamic wavelength tuning characteristics of the 1.5-m three-section DBR lasers: analysis and experiment," *IEEE J. Quantum Elect.*, vol. 31 no. 8, pp. 1389–1400, Aug. 1995.
[27] M. P. Minneman, J. Ensher, M. Crawford, and D. Derickson, "All-semiconductor high-speed akinetic swept-source for OCT," *Proc. SPIE*, vol. 8311 no. 1, pp. 1–10, 2011.
[28] M. Bonesi *et al.*, "Akinetic all-semiconductor programmable swept-source at 1550 nm and 1310 nm with centimeters coherence length," *Opt Exp.*, vol. 22 no. 3, pp. 2632–2655, 2014.
[29] I. Grulkowski *et al.*, "Retinal, anterior segment and full eye imaging using ultrahigh speed swept source OCT with vertical-cavity surface emitting lasers," *Opt. Exp.*, vol. 3 no. 11, pp. 2733–2751, 2012.
[30] M. J. R. Heck and J. E. Bowers, "Integrated Fourier-domain mode-locked lasers: analysis of a novel coherent comb laser," *IEEE J. Sel. Topics Quantum Electron.*, vol. 18 no. 1, pp. 201–209, Jan./Feb. 2012.
[31] R. Huber, M. Wojtkowski, and J. Fujimoto, "Fourier Domain Mode Locking (FDML): A new laser operating regime and applications for optical coherence tomography," *Opt. Exp.*, vol. 14 no. 8, pp. 3225–3237, 2006.
[32] C. M. Eigenwillig *et al.*, "Picosecond pulses from wavelength-swept continuous-wave Fourier domain mode-locked lasers," *Nature Commun.* vol. 4, no. 5, p. 1848, 2013.
[33] X. Gan *et al.*, "Chip-integrated ultrafast graphene photodetector with high responsivity," *Nature Photon.* vol. 7, pp. 883–887, 2013.
[34] H. G. Bach *et al.*, "InP-based waveguide-integrated photodetector with 100-GHz bandwidth," *IEEE J. Sel. Topics Quantum Electron.*, vol. 10, no. 4, pp. 668–672, Jul./Aug. 2004.
[35] W. H. Long, D. H. Mooney, and W. A. Skillman, *Radar Handbook*. New York, NY, USA: McGraw-Hill, 1990.